



Published in final edited form as:

Neuron. 2023 October 04; 111(19): 3119–3130.e4. doi:10.1016/j.neuron.2023.06.015.

Memory-related processing is the primary driver of human hippocampal theta oscillations

Sarah Seger¹, Jennifer Kriegel², Brad Lega³, Arne Ekstrom^{1,2,4,5,*}

¹Neuroscience Interdisciplinary Program, University of Arizona, 1503 E. University Blvd., Tucson, AZ 85719

²Department of Neurosurgery, University of Texas Southwestern Medical School, Dallas, TX

³Psychology Department, University of Arizona, 1503 E. University Blvd., Tucson, AZ 85719

⁴Evelyn McKnight Brain Institute, University of Arizona, 1503 E. University Blvd., Tucson, AZ 85719

⁵Lead Contant

Abstract

Decades of work in rodents suggest that movement is a powerful driver of hippocampal low-frequency “theta” oscillations. Puzzlingly, such movement-related theta increases in primates are less sustained and of lower frequency, leading to questions about their functional relevance. Verbal memory encoding and retrieval lead to robust increases in low-frequency oscillations in humans and one possibility is that memory might be a stronger driver of hippocampal theta oscillations in humans than navigation. Here, neurosurgical patients navigated routes and then immediately mentally simulated the same routes while undergoing intracranial recordings. We found that mentally simulating the same route that was just navigated elicited oscillations that were of greater power, higher frequency, and longer duration than those involving navigation. Our findings suggest that memory is a more potent driver of human hippocampal theta oscillations than navigation, supporting models of internally-generated theta oscillations in the human hippocampus.

eToc

Low frequency “theta” oscillations are strongly linked to movement in the rodent hippocampus but are more transient in humans. By directly comparing the prevalence of human hippocampal

*Correspondence concerning this article should be addressed to Arne Ekstrom, Psychology Department, University of Arizona. adekstrom@arizona.edu.

Author Contributions

Conceptualization, A.D.E., B.L. and S.S.; Methodology, A.D.E., B.L., and S.S.; Investigation, S.S. and J.K.; Writing –A.D.E., S.S., and B.L.; Funding Acquisition, A.D.E.; Resources, A.D.E and B.L.; Supervision, A.D.E and B.L.

Declaration of Interests

The authors declare no competing interests.

Publisher's Disclaimer: This is a PDF file of an article that has undergone enhancements after acceptance, such as the addition of a cover page and metadata, and formatting for readability, but it is not yet the definitive version of record. This version will undergo additional copyediting, typesetting and review before it is published in its final form, but we are providing this version to give early visibility of the article. Please note that, during the production process, errors may be discovered which could affect the content, and all legal disclaimers that apply to the journal pertain.

theta oscillations during navigation and episodic simulation, Seger et al. show that memory is the primary driver of human hippocampal theta oscillations.

Keywords

spatial cognition; navigation; learning; virtual reality

Introduction

Low-frequency, semi-periodic fluctuations in the local field potential of the rodent hippocampus (3–12 Hz) have been linked strongly to voluntary movements^{1–6}, suggesting a tight coupling between sensorimotor driven behavior that occurs during navigation and hippocampal theta oscillations⁷. Invasive recordings in patients undergoing seizure monitoring have also revealed transient bouts of hippocampal theta oscillations during virtual navigation^{8–13} and non-invasively (but less precisely localized) in healthy human participants^{14–16}. These findings support a relationship between theta oscillations and the sensorimotor integration that is present during navigation^{17,18}, although such semi-periodic fluctuations in the local field potential are less sustained and of lower frequency than those typically recorded in rodents¹⁹. Notably, verbal encoding tasks employed to study episodic memory, such as freely recalling or recognizing a list of words, which involve no explicit sensorimotor or movement-related processing, elicit robust hippocampal theta oscillations^{20–22}. Therefore, an important question to address is whether the theta oscillations observed during navigation, which are linked to self-motion and sensory processing, share similar properties to those observed during memory tasks when directly contrasted in the same experiment when controlling for content. Here, we directly test this idea by comparing bouts of navigation in virtual reality with mental simulation of those same routes in patients with electrodes implanted in the hippocampus.

Determining whether the sensorimotor or memory-related processing is the primary correlate of human hippocampal theta oscillations directly relates to another important question: to what extent is external input, in the form of sensory rhythmicity combined with its affiliated self-motion signals, central to the emergence of oscillations? Several theoretical models suggest that hippocampal theta might arise through the integration of sensory and motor components during navigation, and is termed “the sensorimotor integration hypothesis”⁷. Other models suggest that oscillations derive more generally through a process of “active sensing” whereby rhythmic processing of the sensory stimuli entrains oscillations at similar frequencies and harmonics^{23–25}. A common theme across these models is that theta oscillations are related to externally directed sensorimotor processing. Yet, the presence of oscillations during verbal memory encoding and retrieval in humans, in which there is no obvious sensorimotor rhythmicity due to a lack of sustained external cues, present somewhat of an issue for such theoretical models. In addition, a recent study demonstrated that hippocampal theta oscillations persist during periods of teleportation in which no sensory input or motor output is present²⁶. Both memory encoding and teleportation involved relatively brief periods (on the order of seconds) and given that human hippocampal theta oscillations are transient compared to rodents¹⁹, it is possible that the

presence of hippocampal theta oscillations in these studies could be related to lingering signals from interrupted sensory stimuli. In addition, some theoretical models suggest that memory and navigation-related theta may involve different peak frequencies^{27,28}, and therefore directly comparing human hippocampal theta oscillations during navigation and subsequent mental simulation is important to addressing such debates.

To address how navigation and mental simulation-related theta oscillations might compare, we recorded intracranial EEG (iEEG) in patients while they performed a spatial navigation task, with joystick movements and optic flow providing a sense of virtual movement shown to elicit theta oscillations in past studies¹³. Immediately following navigation, patients then mentally simulated the route they just took, placing demands on their memory in the absence of any sensory or self-motion cues. Participants also encoded storefronts they would subsequently experience during navigation and passively viewed a fixation cross as additional control comparisons. We hypothesize that if hippocampal low frequency oscillations are driven by self-motion related to external sensory information (such as in the rodent), we should observe an increase in low frequency oscillations when self-motion is driven by external sensory cues compared to when external sensory and corresponding self-motion cues are absent. In contrast, if hippocampal low frequency oscillations are related to mnemonic processing and are driven strongly by internally-generated activity²⁹, then we expect that low frequency oscillations will increase when memory demand increases.

Results

Comparing navigation with mental simulation behaviorally

To determine whether navigation or mental simulation results in greater low-frequency oscillations, iEEG patients performed a spatial navigation task on a laptop computer using an Xbox controller. As shown in Figure 1a, the spatial navigation task required participants to use a joystick to navigate between stores within a sparse environment (Figure 1d) and subsequently perform mental simulation by “mentally navigating” the route. Mental simulation of each route began upon arrival at the storefront of the target destination and occurred as patients stared at a black screen with a white crosshair (i.e., in the absence of sensory input) and without movement of the joystick (Figure 1a; see Methods). To determine whether patients mentally simulated the routes in a comparable way to the same route they had just navigated, we calculated the linear correlation between the duration for each navigation trial and the duration for each mental simulation trial using a robust regression (Figure 1b; Supplemental Figure 1a). The median rate of compression, which is the ratio of time to navigate a route divided by the time to replay a route, was significantly greater than 1 (Wilcoxon signrank test $p < 0.001$, median navigation / mental simulation = 3.43, Figure 1c). We performed an additional control experiment involving healthy participants who performed the same experiment but involved additional catch trials (see Methods; Supplemental Figure 1c-f) in which they moved the joystick in concert with their mentally simulated route. Healthy controls showed a significant correlation between the duration of navigation and mental simulation (Wilcoxon signrank $p < 0.001$; Supplemental Figure 1c) and a significant correlation between the path tortuosity for navigation and mental simulation catch trials (Wilcoxon signrank $p < 0.001$; Supplemental Figures 1e,f)³⁰. These

analyses, and additional analyses performed on the patient data, support the inference that patients mentally simulated the routes in a comparable way to the same route they had just navigated and is consistent with past work showing similar results³¹.

Mental simulation elicits significant increases in theta oscillatory power compared to control conditions

Inspection of brain recordings from the hippocampus during navigation and mental simulation revealed prominent examples of bouts of low-frequency oscillations, particularly during mental simulation (Figure 1e). To initially compare the presence of low frequency activity during conditions of interest, we computed the power spectral density (PSD) for frequencies between 2–32 Hz and used two one-tailed Wilcoxon rank sum tests (left-tailed and right-tailed) at each frequency. We used the false discovery rate (FDR) to correct for comparisons across multiple frequencies. We compared the median PSD during periods of mobile navigation and mental simulation with three control conditions, each of which involved variations in either visual stimulation, motor control, and/or explicit memory processing.

We first tested whether the median hippocampal 2 – 32 Hz power spectral density during navigation (when mobile only) and during mental simulation differed from the power spectral density during navigation when immobile, with immobility used as a control comparison in many past studies that have identified movement-related hippocampal theta oscillations^{1,4,6,11,13,17,32}. Across the 2 – 32 Hz range, the proportion of electrodes that showed significantly increased power during mobile compared to immobile periods of navigation (ranksum FDR adjusted $p < 0.05$) was significantly greater than expected by chance (FDR adjusted $p < 0.05$; Figure 2a, b; Supplemental Table 1). In contrast, no electrodes showed significantly greater power during immobility compared to mobility (Figure 2a). Our findings therefore replicate past findings showing that oscillatory power is increased during periods of mobility compared to periods of immobility during navigation^{1,4,6,11,13,17,32}. Similarly, across the 2 – 32 Hz range, the proportion of electrodes that showed significantly increased power during mental simulation compared to immobile periods of navigation (ranksum FDR adjusted $p < 0.05$) was significantly greater than expected by chance (FDR adjusted $p < 0.05$; Figure 2c, d; Supplemental Table 1); again, there were no electrodes that showed significantly greater power during immobility compared to mental simulation. Numerically, we found a greater proportion during mental simulation (Figure 2a, green line) compared to navigation (Figure 2c, blue line); we directly compare navigation and mental simulation in the next sections. We also performed all of the analyses above but at the subject level; all of these analyses remained significant (FDR adjusted $p < 0.05$; Supplemental Figure 2e,f).

Next, we compared the median low-frequency power during navigation and mental simulation to the power computed during viewing of static images of the target stores before patients entered the virtual environment (Figure 1a, Storefront Presentation). During storefront presentation, visual stimulation contributes to memory encoding, but joystick-related motor control does not. Importantly, the participant has not entered the environment and memory-related processing is unlikely to contain movement-related information

(although it may involve memory-related rehearsal of the store fronts). We found that in the 2.4 – 3.1 Hz range, navigation elicited significantly greater power than storefront viewing (ranksum FDR adjusted $p < 0.05$) for significantly more electrodes than expected by chance; while in the 14.6 – 19 Hz range, storefront viewing elicited significantly greater power than navigation (ranksum FDR adjusted $p < 0.05$) for significantly more electrodes than expected by chance (Figure 2e, f; Supplemental Table 1). In contrast, for the comparison between storefront viewing and mental simulation, we found a different pattern, namely, in the 2.0 – 2.4 and 5.2 – 14.6 Hz ranges, a significantly greater proportion of electrodes (FDR adjusted $P < 0.05$) showed significantly greater power during mental simulation compared to storefront presentation (Figure 2g, h; Supplemental Table 1). These effects, while trending in the correct direction, did not survive subject-level analyses (FDR adjusted $p > 0.05$; Supplemental Figure 2g,h).

Lastly, we also compared the median power during navigation and mental simulation with that during the crosshair presented between each storefront image (Figure 1a, Crosshair). During the crosshair presentation, neither visual stimulation nor joystick-related motor activity contributes to memory processing although participants may be retrieving storefronts or rehearsing them during this time. The results for the comparison to the crosshair condition were similar to the comparison to the storefront presentation for the electrode level; the crosshairs $>$ navigation contrast was also significant at the subject level (See Supplemental Figure 2a-d,i-j). Mental simulation, possibly due to its high memory demands, induced greater low frequency power than either encoding store fronts or looking at a black screen; surprisingly, navigation appeared to induce similar or less theta power compared to encoding storefronts and looking at a black screen.

Mental simulation elicits greater low-frequency theta activity than during navigation

To directly compare oscillatory power during navigation and mental simulation for each route, we computed the power for frequencies between 2 – 32 Hz during navigation and mental simulation. To account for differences related to the duration of navigation and mental simulation trials, the duration of navigation was matched to the duration of mental simulation on a trial-by-trial basis by selecting a random interval from navigation equal to the length of mental simulation. The proportion of electrodes with a significant increase in power during mental simulation compared to navigation was significantly greater than expected by chance (computed for all frequencies between 2 – 32 Hz, signrank FDR adjusted $p < 0.05$; Figure 3a, b; Supplemental Table 2)²⁷. All of these effects remained significant when performed at the subject-level (Supplemental Figure 3a).

To ensure the robustness of our findings and extension to the domain of semi-periodic signals, we used the eBOSC package to determine the percent of time that power exceeded the aperiodic background activity for at least 3 cycles (termed P_{episode}). By requiring the power to remain above the aperiodic background (i.e., the power threshold) for a minimum of 3 cycles, we were able to isolate and directly compare the prevalence of sustained oscillatory activity during navigation and mental simulation trials at each frequency^{33,34}. Because our earlier analyses had revealed the lowest oscillatory activity during immobility, we used the power during immobility to estimate the background spectrum. We found

that the proportion of electrodes that showed significant increases in the prevalence of oscillations during mental simulation compared to navigation (signrank FDR adjusted $p < 0.05$) was also significantly greater than expected by chance for all frequencies from 2 – 32 Hz (Figure 3c, d; Supplemental Table 2). These effects were also significant at the subject-level (Supplemental Figure 3b). When we performed the same analyses but did not match trial duration, there was again a greater proportion of electrodes with significantly more oscillatory activity during mental simulation compared to navigation from 5.2 – 13.5 Hz and at 20.8 Hz, and, interestingly, a significantly greater proportion of electrodes at 2.4 Hz during navigation than mental simulation (Supplemental Figure 3c); these effects were also robust at the subject-level.

Given the observation that the power spectral density and P_{episode} during mental simulation was significantly higher than navigation for all frequencies between 2 – 32 Hz (Figure 3a), we next controlled for the possibility that a broadband shift in the in the background power spectrum might account for the observed differences in oscillatory prevalence³⁵. We computed the power threshold for P_{episode} separately for navigation and mental simulation, with the average power during each condition serving as its own threshold (“condition-based” baseline, see Methods). This required that oscillatory activity during each condition was greater than the estimate of background activity present during that condition. For frequencies 3.1–3.4 Hz and 4.0 – 24.7 Hz, the proportion of electrodes that showed significantly increased power during mental simulation compared to navigation (signrank FDR adjusted $p < 0.05$) was significantly greater than expected by chance (Supplemental Figure 3d). Thus, after accounting for the differences in the background power spectrum, we found that mental simulation was a stronger driver of low frequency oscillatory activity in the hippocampus than navigation.

To ensure we matched bouts of oscillations between navigation and mental simulation, we randomly selected an interval that was the length of a single cycle from the time points the P_{episode} threshold was passed for each trial and electrode (see Methods). We found that for frequencies 2.6 – 2.8 Hz, 6.2 – 8.7 Hz, and 24.7–32.0 Hz, the proportion of electrodes that showed significantly increased oscillatory power during mental simulation compared to navigation (Wilcoxon signrank FDR adjusted $p < 0.05$) was significantly greater than expected by chance (see Supplemental Figure 3e). We also ran a general linear model comparing P_{episode} (as a dependent variable) with mental simulation and navigation as independent variables across all electrodes; for all frequencies between 2 – 32 Hz, we found that mental simulation explained more variance in P_{episode} across all electrodes than did navigation (see Supplemental Figure 3f).

Mental simulation results in increases in oscillatory frequency and duration compared to navigation

Previous studies have reported a positive relationship between the speed of movement during navigation and the theta frequency^{1,2}. Because our behavioral findings (Figure 1b, c; Supplemental Figure 1d) suggested that the rate at which participants mentally replayed was faster than the rate during navigation, it is possible that at least some of our effects could be due to an increase in the frequency of theta activity during mental simulation. To

determine whether there were frequency shifts between navigation and mental simulation in the theta range, we defined the “peak frequency” for each trial and each condition as the frequency between 2 – 12 Hz when P_{episode} (computed using immobility as baseline) had the highest peak (see Methods). The median electrode-level difference in the peak frequency between navigation and mental simulation was significantly different than zero across electrodes (signrank $p < 0.0001$, median difference = -0.37 Hz; Figure 4a, light orange indicates all electrodes). When we tested the trial-level peak frequency separately for each electrode, 35.5% of electrodes had a peak difference that was significantly greater than zero (Wilcoxon signrank $p < 0.05$; Figure 4a, dark orange). Of the electrodes that had a significant difference in the peak frequency, the proportion that showed a significant increase in the peak frequency during mental simulation was significantly greater than expected by chance ($\chi^2(\text{df} = 1, N = 31) = 40.32$, $p < 0.001$, 32.1% $f_{\text{sim.}} > f_{\text{nav.}}$ and 3.4% $f_{\text{sim.}} < f_{\text{nav.}}$). The result was similar when we computed the peak frequency for the P_{episode} computed with the “condition-based” baseline (data not shown). These results suggest that when a frequency shift was present between navigation and mental simulation, the oscillatory activity during mental simulation occurred at a higher frequency than navigation.

Previous studies have additionally suggested there are two distinct theta oscillations – a higher frequency oscillation (~ 8 Hz) that is associated with spatial-processing and is correlated with movement speed and a separate lower frequency oscillation (~ 3 Hz) that is associated with non-spatial cognitive processes²⁷. Therefore, we also tested the for a shift in the peak frequency separately for 2 – 4 Hz and 5 – 12 Hz (see Methods); we did not find evidence for separate (bimodal) frequency shifts (see Supplemental Figure 3a-d). While the median frequency difference across all electrodes was less than 1Hz, the difference in peak frequency between navigation and mental simulation exhibited much greater variability at the trial level. To address whether there was a relationship between the behavioral compression rate and the difference in peak frequency, we ran a robust regression between the frequency shift and compression rate across all trials separately for each electrode. The number of electrodes ($n = 2$) that showed a significant correlation between the compression rate and the frequency shift within the 2 – 14 Hz range was not significantly greater than that expected by chance (data not shown). These results suggest that our findings did not arise from anterior vs. posterior differences in peak frequencies for navigation compared to simulation and that the small increase in frequency did not relate to the almost three-fold increase in the duration of navigation compared to mental simulation.

Given that we observed an increase in the peak frequency during mental simulation for a significant number of electrodes, one possibility is a narrowband shift in frequency could account for the significant increase found in P_{episode} during mental simulation^{35,36}. To address this question, we tested whether the presence of a significant difference in peak frequency across the 2 – 12 Hz range was associated with the presence of P_{episode} differences between navigation and mental simulation over the same frequency range. We did this by running a Fisher’s Exact test on the number of electrodes that showed significant differences in the P_{episode} during navigation and mental simulation compared to the number that showed a significant difference in peak frequency (see Methods). Only a small number of electrodes that showed a P_{episode} difference also showed a frequency shift, and there was no association between the presence of frequency differences and the presence of P_{episode}

differences (Fisher exact test $p = 1.000$; Figure 4b). In other words, the presence of a frequency shift between navigation and mental simulation at the electrode level did not account for the observed P_{episode} differences.

While the analyses so far suggest that mental simulation resulted in an increase in the peak frequency of theta oscillations compared to navigation, these analyses do not address the duration of these oscillations, with previous studies suggesting that human movement-related theta oscillations are of shorter duration, on average, than rodents¹⁹. This issue is important to understanding the differences in low frequency oscillations during mental simulation compared to navigation and any potential inter-species differences due to memory vs. navigation. To determine the duration that oscillations persisted at each frequency during navigation and mental simulation, we computed P_{episode} for increasing cycle duration criteria from 1 to 4 cycles for each electrode and subsequently computed the cycle duration at which P_{episode} reached its 50% threshold (see Methods). Across electrodes, we found that oscillations were significantly more continuous (i.e., longer in duration) during mental simulation than during navigation at all frequencies between 2 – 32 Hz (Figure 4c). The frequency with the longest duration oscillations during both navigation and mental simulation was 8.0 Hz (median navigation = 2.78 cycles, median mental simulation = 3.18 cycles).

Greater prevalence of low frequency oscillations during later periods of mental simulation and navigation, consistent with more stabilized memory representations

Because learning occurs over the course of the experiment, a *de novo* prediction is that low frequency oscillations during navigation and mental simulation should increase when memory representations are strengthened as a function of experience. In other words, memories should be stronger based on greater experience navigating, thus increasing the fidelity of mental simulations, and possibly navigation, later during learning, resulting in greater detected theta oscillations. To test this hypothesis, we compared the oscillatory prevalence for early versus late trials for navigation and mental simulation (see Methods). For all frequencies between 2 – 32 Hz, we found that the proportion of electrodes that showed a significant increase (signrank FDR adjusted $p < 0.05$) in P_{episode} during late navigation compared to early navigation was significantly greater than expected by chance (Figure 5a; Supplemental Table 3). The proportion of electrodes showing significantly greater power during late relative to early mental simulation was also greater than chance at 2.0 – 2.4 Hz and 4.0 – 16.0 Hz (adjusted $p < 0.05$; Figure 5b; Supplemental Table 3); the proportions of electrodes showing the late > early effect was similar for navigation. The presence of a significant increase in the prevalence of theta oscillations during late trials of navigation and mental simulation compared to early trials support the conclusion that an increase in the strength of memory representations results in an increase in the presence of theta oscillations. We performed additional analyses to address whether this early versus late difference in theta oscillations might be related to differences in encoding and retrieval, which might also contribute to theta oscillations. We found that when comparing both early and late simulation trials to early and late trials during navigation, early and late simulation trials elicited greater theta activity than early and late navigation trials (Supplemental Figure 5). We also found that little new learning occurred during the Navigation and Simulation

blocks (see Methods and Supplemental Figure 1b), suggesting that encoding and retrieval demands should be relatively balanced for our comparisons of navigation and simulation. Together, these analyses suggested that the differences in theta oscillations for early vs. late trials was unlikely to be accounted for by encoding versus retrieval differences alone.

Greater prevalence of low frequency oscillations for simulation vs. navigation in the posterior hippocampus but no difference in a control brain region

We next tested whether electrodes located in the anterior versus posterior hippocampus (see Methods) showed differences in the prevalence of low frequency oscillations during navigation and mental simulation, as past reports have suggested differences in anterior vs. posterior hippocampus based on memory and navigation²⁷. The proportion of electrodes that showed significantly greater P_{episode} during navigation compared to mental simulation (i.e., navigation > simulation) was not significantly different for the anterior versus posterior hippocampus (Figure 6a; Supplemental Table 4). During mental simulation, however, we did find a significant difference in the proportion of electrodes that showed significantly greater P_{episode} in the anterior versus posterior hippocampus. The proportion of electrodes with significantly increased power during simulation in the posterior hippocampus was significantly greater than the anterior hippocampus for frequencies 8.7 – 10.3 Hz and at 22.6 Hz (Wilcoxon ranksum $p < 0.05$). However, these effects did not survive FDR correction. We also compared the duration of oscillations in the anterior versus the posterior during navigation and simulation and found no significant differences (See Supplemental Figure 6).

To determine whether the increase in the prevalence of low frequency oscillations during mental simulation was specific to the hippocampus, we repeated the comparison between the P_{episode} during navigation versus mental simulation for electrodes that were localized to the anterior cingulate cortex, an area with numerically the closest number of electrodes to the hippocampus. For the P_{episode} (Figure 6c; Supplemental Table 4), we found electrodes that showed significant differences (signrank FDR adjusted $p < 0.05$) during navigation and mental simulation (Figure 6c), although this proportion was markedly lower than what we observed in the hippocampus (Figure 3c). In addition, the proportion of electrodes that showed significantly greater P_{episode} during one condition did not significantly differ from the proportion showing the effect for the opposite condition (FDR adjusted $p > 0.05$).

Discussion

Here, we used a novel spatial navigation task that included joystick-based navigation and mental simulation of the same routes to compare low-frequency oscillations when controlling for content. During navigation, sensorimotor processing is directed externally, with any memory-related demands strongly driven by external sensory cues experienced during self-motion. In contrast, during mental simulation, there is no externally directed sensorimotor integration and all internal processes must be guided primarily by memory-related processing. By comparing low frequency oscillations during navigation and mental simulation during control conditions that varied memory processing and visual stimulation (i.e., encoding store fronts and viewing a fixation cross during inter-trial intervals), we found an increase in low frequency oscillations even in the absence of externally directed

sensorimotor processing. When we directly compared low frequency oscillations during navigation to mental simulation of the same route, we found that mental simulation induced greater low-frequency oscillations on the electrode and subject level. This was true for both early and late trials of mental simulation compared to navigation (Supplemental Figure 5), suggesting that the difference was unlikely to be due to differences in demands on encoding and retrieval. On the electrode level, both differences in frequency-specific power (power shifts) and differences in the peak frequency (narrowband frequency shifts) contributed to the differences in low frequency oscillations, although the majority of increases that we observed in theta activity during mental simulation could not be accounted for by broad-band frequency shifts. Overall, mental stimulation resulted in increases in the duration, power, and frequency of detected oscillations when controlling for differences in their relative durations. These results therefore suggest that semi-periodic increases in low-frequency oscillations are elicited by mental simulation, even in the absence of any external sensory or self-motion cues, and in a manner that is stronger than those elicited during navigation.

Decades of evidence from rodent studies have found that low frequency oscillations are associated with voluntary self-motion in an environment¹⁻⁶. Comparatively, however, low-frequency oscillations during virtual navigation in humans are of lower frequency and less continuous¹⁹, leading to the suggestion that theta oscillations may be of lower frequency in humans than rodents²⁸, possibly differ in anterior vs. posterior hippocampus based on self-motion²⁷, or are simply harder to observe³⁷. One factor that might contribute to the differences between humans and rats in terms of theta oscillations during navigation is that most rodent studies involve navigation with the full-range of body-based cues (i.e., head rotations and walking cues) although human patient studies typically involve navigation in virtual reality. One experiment that directly contrasted virtual with real-world ambulation, however, reported only modest increases in frequency and oscillatory prevalence⁹ during real-world navigation (see also⁸). Notably, recordings in non-human primates during unrestrained real-world navigation have also reported comparatively less continuous and lower power theta oscillations than what is typically reported in rodents^{38,39}. This suggests that the addition of vestibular and body-based cues is unlikely to account for the difference in the prevalence of low-frequency oscillations in the hippocampus between primates in rodents. Additionally, another factor that might contribute to the differences for theta oscillations during navigation between rats and humans are differences in how information is acquired during navigation from the sensory systems. Rodents show a strong coupling between sniffing and whisking behaviors, which also shows a strong correlation with the prevalence of theta oscillations and relates to active movement⁴⁰. On the other hand, the human visual system provides higher-acuity spatial information about the external environment compared to rodents⁴¹, with attention to visual input correlating strongly with the emergence of oscillations²⁴. Based on the lower prevalence of low-frequency hippocampal oscillations with self-motion in primates versus rats, one possibility, then, is that theta oscillations are less functionally relevant to self-motion in primates than in rodents due to differences in the acuity of our visual systems and the relationship of eye movements, while stationary, to exploration^{41,42}.

By directly pitting periods of movement during navigation against the same periods during mental simulation in the absence of visual-sensory cues or explicit motor movements, we could directly compare the two signals. In the absence of movement during periods of immobility, we found greatly reduced low-frequency oscillatory activity, with movement resulting in some increases in theta oscillations, replicating past studies^{1,4,6,11,13,17,32}. This increase, however, was dwarfed by the increase in theta oscillations during mental simulation, a situation in which participants had no external sensory input to indicate movement. These findings thus suggest that memory-related processing, which would likely have greater demands during mental simulation than navigation, is a stronger driver of human hippocampal theta than navigation. Consistent with this, we observed higher prevalence of theta during later periods of navigation and mental simulation, when memory traces would likely be stronger and of higher fidelity. Our results therefore help to potentially resolve the debate about why primate hippocampal oscillations are sometimes observed to be less prevalent than rodents by suggesting that memory-related processing is a stronger driver of low-frequency hippocampal oscillations than self-motion in humans.

Notably, a parallel literature has identified low-frequency oscillations during variegated memory processing, including recognizing words, freely recalling words, and non-verbal source memory tasks^{20–22,43}. Of note, however, is a line of research suggesting that it is not movement itself that is necessary for place cell and theta activity but rather the intention or sense of movement^{29,44}. For example, the original formulation from Vanderwolf suggested that voluntary intention was a driver of theta and not necessarily movement itself⁶. Theta oscillations in humans are also present during teleportation in the absence of any sensory or motor demands, suggesting that some aspects may be internally-generated and not dependent on external signals²⁶. Hippocampal theta oscillations are also present in both humans and rats during some sleep stages (e.g., REM sleep)^{45,46}, providing additional support for the conclusions that external sensory input is not critical to elicit hippocampal theta oscillations. Taken together, this evidence suggests that internal context (that is context that exists internally, which might or might not be directly related to the external environment), is a strong driver of memory-based processing in the hippocampus (see also^{47,48}). We also observed greater theta oscillations for viewing cross-hairs than virtual navigation, when there were no external self-motion cues but potentially higher demands on memory retrieval and other internally generated processing, with this control condition showing less theta activity than mental stimulation. The presence of theta oscillations during the cross-hairs and mental simulation periods is also consistent with a well-developed literature suggesting the importance of low-frequency oscillations to resting state and the default mode network⁴⁹. Because we did not look at coupling between other brain regions in this study, however, we cannot definitively link our findings to this work. One potential way to address the issue of whether theta oscillations are driven primarily by mnemonic content or simply being in a resting state would be to compare mental simulation before navigation, when presumably mnemonic content is lower, to mental simulation after navigation, when mnemonic content is likely higher.

A recent study by Goyal et al. suggested that hippocampal theta oscillations might differ by task as a function of anterior vs. posterior hippocampal recording sites. This study found that oscillations related to spatial-related processing occurred at a faster frequency (~8

Hz) and were more robust in the posterior compared to anterior hippocampus. In contrast, hippocampal theta oscillations related to non-spatial-related processing were slower (~3 Hz) and more robust in the anterior hippocampus than posterior hippocampus. Thus, one possibility could be that the greater prevalence of theta activity we observed during mental simulation compared to navigation could have reflected implant location rather than a functional difference. The implantations in this study, like in the Goyal et al study, involved placements in both anterior and posterior hippocampus, allowing us to compare the two. Like in the Goyal et al. study, when we compared oscillatory prevalence over the entire trial duration (i.e., when we did not match the duration of navigation and simulation), we found evidence for separate peaks in the oscillatory activity at ~2.4 Hz and at 5.2 – 13.5 Hz (Supplemental Figure 3c), although we did not find an interaction with anterior vs. posterior implant location. When the duration of mental simulation and navigation were matched, however, the prevalence of oscillations centered at both 3 Hz and 8Hz were greater during mental simulation than navigation. Because longer duration epochs could result in greater detection of oscillations, our findings are more consistent with an increase in low-frequency oscillations during memory processing compared to navigation across the longitudinal extent of the hippocampus. Taken together, our findings suggest that memory-related processing results in more robust and sustained increases in low-frequency theta oscillations than sensory-driven movement or navigation.

STAR Methods

RESOURCE AVAILABILITY

Lead Contact—Further information and requests for resources and reagents should be directed to and will be fulfilled by the lead contact, Arne D. Ekstrom (adekstrom@arizona.edu).

Materials Available—This study did not generate new unique reagents.

Data and code availability

- Raw iEEG data that support the conclusions of this study are available for public download on Zenodo: <https://doi.org/10.5281/zenodo.8058006>
- This paper does not report original code. The code used to generate the results presented in this study will be shared by the lead contact upon request.
- Any additional information required to reanalyze the data reported in this paper is available from the lead contact upon request.

EXPERIMENTAL MODEL AND STUDY PARTICIPANT DETAILS

Intracranial EEG Participants—12 patients with medically intractable epilepsy who underwent stereo-electroencephalography surgery for clinical purposes were recruited to participate in this study. Data were collected from the University of Texas Southwestern Medical Center epilepsy program. In total, there were 7 males and 5 females between 21 – 63 years of age (median 41 years old). Each participants provided written informed consent

to participants in the study, which was approved by the University of Texas Southwestern Medical Center Institutional Review Board.

Healthy Participants—13 healthy controls were recruited from the student population at the University of Arizona to complete the modified version of the behavioral at. In total, there were 7 females and 6 males between the ages of 18–24.

METHOD DETAILS

Intracranial EEG Recordings—Each subject was implanted with up to 17 depth electrodes containing 8–16 cylindrical platinum–iridium recording contacts spaced 2–6-mm apart. Electrode placement was dictated solely by the clinical need for seizure localization. Intracranial EEG data were recorded using a Nihon Kohden EEG-1200 clinical system. Signals were sampled at 1000 Hz and referenced to a common intracranial contact.

Electrode Localization—Electrode localization was achieved by co-registration of the post-operative computed tomography scans with the pre-operative magnetic resonance images using the FSL's/FLIRT software⁵⁰. The co-registered images were evaluated by an expert member of the neuroradiology team to determine the final electrode locations. Each subject had at least three recording contacts localized to the hippocampus. The median number of hippocampal contacts per subject was 6. The uncus notch was used to demarcate anterior versus posterior hippocampal location⁵¹. The median number contacts in the anterior hippocampus per subject was 3.5, and the median number in the posterior hippocampus per subject was 2.

Experimental Paradigm—Patients performed a spatial navigation task on a laptop computer using an Xbox controller. In this task, participants navigated routes between stores located within a sparse environment and mentally simulated the routes immediately upon route completion. The task was designed as follows. Before entering the virtual environment, the participant completed the *Storefront Familiarization* portion of the task during which the six storefronts were displayed successively on a blank screen for 5000 milliseconds(ms) to familiarize the participants with the target stores. Between the appearance of each storefront a white crosshair was displayed on a black background for 5000ms. After viewing each storefront 2x, the participant began the *Navigation Only* portion of the task. The *Navigation Only* portion of the task began when the participant appeared outside one of the stores in the virtual environment in a first-person point of view, and a semi-transparent on-screen prompt instructed the participant to locate one of the five remaining target stores. The prompt remained overlaid on the entire screen for 5000ms, during which time the participant was able to begin using the XBox joystick to navigate to the target store. After 5000ms, the on-screen prompt was reduced in size and moved to the top right corner of the screen. Once the participant reached the target store, another semi-transparent on-screen prompt was overlaid on the screen for 5000 ms indicating that the target store was identified. During *Navigation Only*, the prompt indicating the identification of the target store was followed by a white crosshair that was displayed on a black background for 5000ms (e.g. the environment was not visible). Following the

crosshair, the participants' previous view of the environment was restored and a new prompt instructed the participant to locate the next store.

After the participant visited each store 2x, the participant began the *Navigation with Mental Simulation* portion of the task during which the participant was instructed to “mentally navigate” the route upon arrival at the target store (See Instructions for Mental Simulation). The task structure of *Navigation with Mental Simulation* was similar to *Navigation Only*; however, the on-screen prompt that indicated the successful identification of the target store was instead followed by a self-paced on-screen prompt which instructed the participant to press [A] on the controller to begin mental simulation of the route and [A] again to end mental simulation. When the participant pressed [A] to begin mental simulation, the instructions on the screen were replaced by a white crosshair, which the participants were instructed to look at while actively mentally navigating. When the participant pressed [A] to indicate the end of mental simulation, the previous view of the environment was restored and a new on-screen prompt overlaying the environment instructed the participant to locate the next store. This procedure was repeated 44x. For each of the 44 trials, the participant was assigned to one of two speeds--5 vm/s (slow speed) or 8 vm/s (fast speed). On trials in which the participant navigated without mental simulation, the speed of movement was equal to 6 vm/s (medium speed). 10% of the 44 navigation + mental simulation trials consisted of catch trials. The speed manipulation was not considered in this manuscript. On catch trials, the participant was instructed to use the controller to simulate the imagined route during mental simulation. The catch trials were to ensure that participants were actually remembering the route when mentally simulating.

Instructions for mental simulation: After consenting to the task and prior to starting, each participant completed a practice exercise to become familiar with the task design. The practice exercise consisted of asking the participant to imagine standing at home in their bedroom and then imagine walking from this location in the bedroom to the kitchen. All participants were successfully able to complete this exercise before beginning the task.

Instructions for practice task: At the beginning of the task, the participant completed a practice version of the entire task. The practice version of the task was identical to the full version; however, the number of trials was condensed (2 navigation trials, 2 navigation + mental simulation trials) and the virtual environment consisted of 2 stores located on either end of a straight road. There were no catch trials during mental simulation in the practice version of the experiment. The practice version was designed to familiarize participants with the task structure and instructions prior to the experiment.

Modified experimental paradigm: The modified version of the task was identical to the original version of the task except for the number of catch trials during mental simulation—which was increased to 15 total.

Behavioral Performance Metrics

Excess Path: To measure learning throughout the experiment, we computed the excess path, which was defined as the difference between the length of the traveled route and the optimal

route. The length of the optimal route was equivalent to the shortest possible route between two stores. Excess path was computed for all navigation trials.

Tortuosity: Path tortuosity was used to compare the path during navigation and the path during mental simulation catch trials³⁰. Path tortuosity was computed using the straightness index, which is the ratio of the distance between the start and end points and the path length⁵².

Preprocessing—Raw intracranial EEG recordings were subsequently re-referenced to a common average montage, with each contact referenced to the average across all contacts. All analyses were conducted using MATLAB with both built-in and custom-made scripts. We employed an automated artifact rejection algorithm to exclude interictal activity by computing kurtosis over a sliding window of 1000 ms duration and a kurtosis threshold of 5. Prior to analysis, each participant's EEG data was first filtered with a 6th-order highpass Butterworth filter at 1Hz followed by 6th-order bandstop Butterworth filters at 57 – 63 Hz and 117 – 123 Hz to remove line noise.

Data Analysis—For each experimental session, the following time intervals, as shown in Figure 1a, were defined as conditions of interest: crosshair presentation (12 trials, 5000ms duration), storefront presentation during store familiarization (12 trials, 5000ms duration), navigation only (12 trials, variable duration), navigation (44 trials, variable duration), and mental simulation (44 trials, variable duration). For each navigation trial, time points were further broken down into intervals of immobility and mobility, with periods of immobility defined as time intervals with no horizontal motion nor any change in the field of view (no rotation) for a minimum of 500 ms. Trials within the *Navigation with Mental Simulation* block of the experiment were further separated into early trials, which were defined as the first 12 trials, and late trials, defined as the last 12 trials of (Figure 1a).

Because the duration of navigation and mental simulation differed, the duration of navigation was matched to the duration of mental simulation on a trial-by-trial basis by randomly selecting a time interval from navigation that matched the duration of mental simulation for that trial.

Power Spectral Density Estimation—To estimate the power spectral density at log-spaced frequencies between 2–32Hz, a continuous wavelet Morlet transform (width = 6) was computed at every time point for each trial. For each trial in every condition of interest (see data analysis), a single power spectral density estimate was obtained by averaging power estimates across time points. To compute the power spectral density estimates for time periods of mobility (and immobility) for each trial, the power spectral density from navigation was averaged only across time points of mobility (and vice versa for immobility). The navigation, mobile, and immobile, and mental simulation durations varied between 1000ms - 48000 ms on a trial-by-trial basis depending on the speed of navigation and the route traveled. In order to account for differences in the duration of time

extended-Better OSCillation detection (P_{episode})—To further characterize oscillations in the hippocampus during navigation and mental simulation, we used the

extended-Better OSCillation Detection (eBOSC) to determine the duration and power of sustained oscillations in the hippocampus during navigation and mental simulation^{33,34}. More specifically, we computed the fraction of time (P_{episode}), that power is maintained above the power and duration threshold versus the total amount of time.

eBOSC relies on a power and duration threshold to separate rhythmic activity from aperiodic background activity. The power threshold is determined by computing a robust linear fit to the log-log power spectrum across all time points during a “baseline” condition of interest, and the robust linear fit is the estimate of the background spectrum during that condition. The duration threshold results in the detection of sustained oscillation as opposed to transient non-periodic signals that persist for short periods of time. Because we were interested in the rhythmic activity that existed within each condition, the background spectrum was estimated using the power during periods of immobility (immobile-based baseline). We also used a second “baseline” condition for P_{episode} where we calculated the threshold for navigation and mental simulation separately by using the power during each condition itself to serve as its baseline (condition-based baseline).

Because P_{episode} is a ratio of the amount of time that the power spends above the threshold to the total duration of the trial, we matched the duration of navigation and mental simulation for each trial to account for differences related to the longer trial duration for navigation. We also computed the P_{episode} using the full trial length for navigation and mental simulation (Supplemental Figure 3c).

Oscillation Duration Detection—To measure the duration over which oscillation persisted in each condition, we separately computed the P_{episode} using a duration threshold from 1 to 4 cycles, spaced 0.5 cycle apart. For each trial, we interpolated the P_{episode} from 1 to 4 cycles from a resolution of 0.5 cycles to a resolution of 0.1 cycles, separately for each frequency. Then for each trial and at each frequency, we computed the cycle duration at which the P_{episode} was equivalent to 50% of the P_{episode} measured for the duration threshold of 1 cycle¹⁹.

Theta Frequency Range—We defined the theta band as frequencies from 2 – 12 Hz because this was roughly the range over which the PSD (Figure 3a) and P_{episode} (Figure 3c) significantly differed for navigation and mental simulation. The range 2–12 Hz also roughly coincided with the frequencies at which we found differences in the oscillatory power (Supplemental Figure 3b) and the P_{episode} computed with a condition-based baseline (Supplemental Figure 3a).

Peak Frequency Detection—Since we were interested in identifying the frequency with the most oscillatory activity during each condition, we used the P_{episode} computed using the full trial durations with immobility used for the power threshold. MATLABs ‘findpeaks’ function was used to identify the frequency within the 2 – 12 Hz range at which P_{episode} had the largest peak for each trial and each condition. Next, the difference in the peak frequency was computed for each navigation and mental simulation trial.

Past studies have also suggested that there are two distinct theta oscillations in the human hippocampus— a lower frequency oscillation (~3Hz) that is associated with spatial-processing and is correlated with movement speed and a separate higher frequency oscillation (~8 Hz) that is associated with non-spatial and memory-related processes²⁷. In our data, the P_{episode} computed for full navigation duration (Supplemental Figure 3c) shows evidence for a peak around 2.4 Hz during navigation and at about 9 Hz during mental simulation. Therefore, we also split the 2 – 12 Hz into low (2 – 4 Hz) and high (5 – 12 Hz) theta bands and found the peak difference separately for each band.

Single Cycle Oscillation Power—To compare oscillatory power for time periods when power rises above the P_{episode} threshold, for each trial, we computed the median power over a one cycle interval selected randomly from the time point when the P_{episode} power and duration threshold were passed for each trial.

General Linear Model (GLM)—We ran a general linear model comparing the rate that the P_{episode} power and duration threshold was passed (as a dependent variable) with mental simulation and navigation as independent variables. To compute the rate over which P_{episode} power and duration threshold was passed, we first created a binary matrix to indicate all the time points during the task when the P_{episode} power and duration threshold passed for each frequency. We then used a Gaussian kernel with a 1000ms width to generate a continuous measure of the rate over which the P_{episode} threshold was passed. We used MATLAB's "stepwiseglm" function to run a general linear model for each electrode with P_{episode} rate serving as the dependent variable and navigation and mental stimulation serving as the independent variables. We then evaluated the parameter fits (beta values) across all electrodes.

Linear Regressions—All regressions were robust linear regressions performed in MATLAB using the *fitlm* function.

QUANTIFICATION AND STATISTICAL ANALYSIS

Electrode Level Comparisons—To compare the power spectral density (PSD), P_{episode} , peak frequencies, oscillation duration, and single cycle power estimates between conditions for each electrode, we used separate one-tailed non-parametric tests to determine whether the measure was significantly greater in condition 1 (left-tailed) or condition 2 (right-tailed) across trials. For comparisons between navigation and subsequent replay trials, we also used a non-parametric test (Wilcoxon signrank). For comparisons between both navigation and mental simulation either crosshair, storefront, or early / late comparisons, we used a Wilcoxon ranksum test. For each electrode and each comparison, we used the false discovery rate (FDR) to correct the p-values at each frequency for multiple comparisons.

For each comparison of interest, we computed the total fraction of electrodes that showed significantly greater power for condition A relative to condition B, and vice versa (condition B relative to condition A, i.e., navigation PSD > mental simulation PSD). We then used a χ^2 test at each frequency to determine whether there were significant differences in the proportion of electrodes that showed a significant difference for $A > B$ compared to $B > A$.

Because we performed a χ^2 test at each frequency, we again used FDR correction to correct for multiple comparisons. To test the distribution of peak frequencies between navigation and mental simulation across electrodes, we used a Wilcoxon signrank test. To test the distribution of peak frequency differences across trials for each electrode, we again used a Wilcoxon signrank. A Wilcoxon signrank test was used to test the distribution of correlation coefficients to zero. A Fisher exact test was used to determine whether the presence of a significant peak frequency difference was associated with the presence of a significant difference in P_{episode} .

Subject Level Comparisons—To determine whether the power and P_{episode} differences at the electrode level also hold at the subject level, we computed the proportion of subjects with at least one significant electrode during condition A relative to condition B, and vice versa (condition B relative to condition A, i.e., navigation PSD > mental simulation PSD). We then used a χ^2 test at each frequency to determine whether there were significant differences in the proportion of subjects that showed a significant difference for A > B compared to B > A. Because we performed a χ^2 test at each frequency, we again used FDR correction to correct for multiple comparisons.

Supplementary Material

Refer to Web version on PubMed Central for supplementary material.

References

1. Czurkó A, Hirase H, Csicsvari J, and Buzsáki G. (1999). Sustained activation of hippocampal pyramidal cells by ‘space clamping’ in a running wheel. *European Journal of Neuroscience* 11, 344–352. 10.1046/j.1460-9568.1999.00446.x. [PubMed: 9987037]
2. Kennedy JP, Zhou Y, Qin Y, Lovett SD, Sheremet A, Burke SN, and Maurer AP (2022). A Direct Comparison of Theta Power and Frequency to Speed and Acceleration. *J. Neurosci.* 42, 4326–4341. 10.1523/JNEUROSCI.0987-21.2022. [PubMed: 35477905]
3. Kropff E, Carmichael JE, Moser EI, and Moser M-B (2021). Frequency of theta rhythm is controlled by acceleration, but not speed, in running rats. *Neuron* 109, 1029–1039.e8. 10.1016/j.neuron.2021.01.017. [PubMed: 33567253]
4. McFarland WL, Teitelbaum H, and Hedges EK (19750101). Relationship between hippocampal theta activity and running speed in the rat. *Journal of Comparative and Physiological Psychology* 88, 324. 10.1037/h0076177. [PubMed: 1120805]
5. Sheremet A, Burke SN, and Maurer AP (2016). Movement Enhances the Nonlinearity of Hippocampal Theta. *J. Neurosci.* 36, 4218–4230. 10.1523/JNEUROSCI.3564-15.2016. [PubMed: 27076421]
6. Vanderwolf CH (1969). Hippocampal electrical activity and voluntary movement in the rat. *Electroencephalography and Clinical Neurophysiology* 26, 407–418. 10.1016/0013-4694(69)90092-3. [PubMed: 4183562]
7. Bland BH, and Oddie SD (2001). Theta band oscillation and synchrony in the hippocampal formation and associated structures: the case for its role in sensorimotor integration. *Behav Brain Res* 127, 119–136. 10.1016/s0166-4328(01)00358-8. [PubMed: 11718888]
8. Aghajian ZM, Schuette P, Fields TA, Tran ME, Siddiqui SM, Hasulak NR, Tcheng TK, Eliashiv D, Mankin EA, Stern J, et al. (2017). Theta Oscillations in the Human Medial Temporal Lobe during Real-World Ambulatory Movement. *Current Biology* 27, 3743–3751.e3. 10.1016/j.cub.2017.10.062. [PubMed: 29199073]

9. Bohbot VD, Copara MS, Gotman J, and Ekstrom AD (2017). Low-frequency theta oscillations in the human hippocampus during real-world and virtual navigation. *Nat Commun* 8, 14415. 10.1038/ncomms14415. [PubMed: 28195129]
10. Bush D, Bisby JA, Bird CM, Gollwitzer S, Rodionov R, Diehl B, McEvoy AW, Walker MC, and Burgess N. (2017). Human hippocampal theta power indicates movement onset and distance travelled. *Proceedings of the National Academy of Sciences* 114, 12297–12302. 10.1073/pnas.1708716114.
11. Ekstrom AD, Caplan JB, Ho E, Shattuck K, Fried I, and Kahana MJ (2005). Human hippocampal theta activity during virtual navigation. *Hippocampus* 15, 881–889. 10.1002/hipo.20109. [PubMed: 16114040]
12. Ekstrom A, Suthana N, Millett D, Fried I, and Bookheimer S. (2009). Correlation between BOLD fMRI and theta-band local field potentials in the human hippocampal area. *J Neurophysiol* 101, 2668–2678. 10.1152/jn.91252.2008. [PubMed: 19244353]
13. Watrous AJ, Fried I, and Ekstrom AD (2011). Behavioral correlates of human hippocampal delta and theta oscillations during navigation. *Journal of Neurophysiology* 105, 1747–1755. 10.1152/jn.00921.2010. [PubMed: 21289136]
14. Cornwell BR, Arkin N, Overstreet C, Carver FW, and Grillon C. (2012). Distinct contributions of human hippocampal theta to spatial cognition and anxiety. *Hippocampus* 22, 1848–1859. 10.1002/hipo.22019. [PubMed: 22467298]
15. Cornwell BR, Johnson LL, Holroyd T, Carver FW, and Grillon C. (2008). Human Hippocampal and Parahippocampal Theta during Goal-Directed Spatial Navigation Predicts Performance on a Virtual Morris Water Maze. *J. Neurosci.* 28, 5983–5990. 10.1523/JNEUROSCI.5001-07.2008. [PubMed: 18524903]
16. de Araújo DB, Baffa O, and Wakai RT (2002). Theta oscillations and human navigation: a magnetoencephalography study. *J Cogn Neurosci* 14, 70–78. 10.1162/089892902317205339. [PubMed: 11798388]
17. Caplan JB, Madsen JR, Schulze-Bonhage A, Aschenbrenner-Scheibe R, Newman EL, and Kahana MJ (2003). Human θ Oscillations Related to Sensorimotor Integration and Spatial Learning. *J. Neurosci.* 23, 4726–4736. 10.1523/JNEUROSCI.23-11-04726.2003. [PubMed: 12805312]
18. Cruikshank LC, Caplan JB, and Singhal A. (2012). Human electrophysiological reflections of the recruitment of perceptual processing during actions that engage memory. *Journal of Vision* 12. 10.1167/12.6.29.
19. Watrous AJ, Lee DJ, Izadi A, Gurkoff GG, Shahlaie K, and Ekstrom AD (2013). A comparative study of human and rat hippocampal low-frequency oscillations during spatial navigation. *Hippocampus* 23, 656–661. 10.1002/hipo.22124. [PubMed: 23520039]
20. Lega BC, Jacobs J, and Kahana M. (2012). Human hippocampal theta oscillations and the formation of episodic memories. *Hippocampus* 22, 748–761. 10.1002/hipo.20937. [PubMed: 21538660]
21. Sederberg PB, Kahana MJ, Howard MW, Donner EJ, and Madsen JR (2003). Theta and gamma oscillations during encoding predict subsequent recall. *J Neurosci* 23, 10809–10814. 10.1523/JNEUROSCI.23-34-10809.2003. [PubMed: 14645473]
22. Solomon EA, Kragel JE, Sperling MR, Sharan A, Worrell G, Kucewicz M, Inman CS, Lega B, Davis KA, Stein JM, et al. (2017). Widespread theta synchrony and high-frequency desynchronization underlies enhanced cognition. *Nat Commun* 8, 1704. 10.1038/s41467-017-01763-2. [PubMed: 29167419]
23. Lakatos P, Chen C-M, O'Connell MN, Mills A, and Schroeder CE (2007). Neuronal oscillations and multisensory interaction in primary auditory cortex. *Neuron* 53, 279–292. 10.1016/j.neuron.2006.12.011. [PubMed: 17224408]
24. Lakatos P, Karmos G, Mehta AD, Ulbert I, and Schroeder CE (2008). Entrainment of Neuronal Oscillations as a Mechanism of Attentional Selection. *Science* 320, 110–113. 10.1126/science.1154735. [PubMed: 18388295]
25. Schroeder CE, Wilson DA, Radman T, Scharfman H, and Lakatos P. (2010). Dynamics of Active Sensing and perceptual selection. *Curr Opin Neurobiol* 20, 172–176. 10.1016/j.conb.2010.02.010. [PubMed: 20307966]

26. Vass LK, Copara MS, Seyal M, Shahlaie K, Farias ST, Shen PY, and Ekstrom AD (2016). Oscillations Go the Distance: Low-Frequency Human Hippocampal Oscillations Code Spatial Distance in the Absence of Sensory Cues during Teleportation. *Neuron* 89, 1180–1186. 10.1016/j.neuron.2016.01.045. [PubMed: 26924436]
27. Goyal A, Miller J, Qasim SE, Watrous AJ, Zhang H, Stein JM, Inman CS, Gross RE, Willie JT, Lega B, et al. (2020). Functionally distinct high and low theta oscillations in the human hippocampus. *Nature Communications* 11, 2469. 10.1038/s41467-020-15670-6.
28. Jacobs J. (2014). Hippocampal theta oscillations are slower in humans than in rodents: implications for models of spatial navigation and memory. *Philos Trans R Soc Lond B Biol Sci* 369, 20130304. 10.1098/rstb.2013.0304. [PubMed: 24366145]
29. Wang Y, Romani S, Lustig B, Leonardo A, and Pastalkova E. (2015). Theta sequences are essential for internally generated hippocampal firing fields. *Nat Neurosci* 18, 282–288. 10.1038/nn.3904. [PubMed: 25531571]
30. Daugherty AM, Yuan P, Dahle CL, Bender AR, Yang Y, and Raz N. (2015). Path Complexity in Virtual Water Maze Navigation: Differential Associations with Age, Sex, and Regional Brain Volume. *Cereb Cortex* 25, 3122–3131. 10.1093/cercor/bhu107. [PubMed: 24860019]
31. Arnold AEGF, Iaria G, and Ekstrom AD (2016). Mental simulation of routes during navigation involves adaptive temporal compression. *Cognition* 157, 14–23. 10.1016/j.cognition.2016.08.009. [PubMed: 27568586]
32. Ekstrom AD, Kahana MJ, Caplan JB, Fields TA, Isham EA, Newman EL, and Fried I. (2003). Cellular networks underlying human spatial navigation. *Nature* 425, 184. 10.1038/nature01964. [PubMed: 12968182]
33. Hughes AM, Whitten TA, Caplan JB, and Dickson CT (2012). BOSC: a better oscillation detection method, extracts both sustained and transient rhythms from rat hippocampal recordings. *Hippocampus* 22, 1417–1428. 10.1002/hipo.20979. [PubMed: 21997899]
34. Whitten TA, Hughes AM, Dickson CT, and Caplan JB (2011). A better oscillation detection method robustly extracts EEG rhythms across brain state changes: the human alpha rhythm as a test case. *Neuroimage* 54, 860–874. 10.1016/j.neuroimage.2010.08.064. [PubMed: 20807577]
35. Herweg NA, Solomon EA, and Kahana MJ (2020). Theta Oscillations in Human Memory. *Trends in Cognitive Sciences* 24, 208–227. 10.1016/j.tics.2019.12.006. [PubMed: 32029359]
36. Manning JR, Jacobs J, Fried I, and Kahana MJ (2009). Broadband Shifts in Local Field Potential Power Spectra Are Correlated with Single-Neuron Spiking in Humans. *Journal of Neuroscience* 29, 13613–13620. 10.1523/JNEUROSCI.2041-09.2009. [PubMed: 19864573]
37. Skaggs WE, McNaughton BL, Permenter M, Archibeque M, Vogt J, Amaral DG, and Barnes CA (2007). EEG sharp waves and sparse ensemble unit activity in the macaque hippocampus. *J Neurophysiol* 98, 898–910. 10.1152/jn.00401.2007. [PubMed: 17522177]
38. Courellis HS, Nummela SU, Metke M, Diehl GW, Bussell R, Cauwenberghs G, and Miller CT (2019). Spatial encoding in primate hippocampus during free navigation. *PLOS Biology* 17, e3000546. 10.1371/journal.pbio.3000546.
39. Mao D, Avila E, Caziot B, Laurens J, Dickman JD, and Angelaki DE (2021). Spatial modulation of hippocampal activity in freely moving macaques. *Neuron* 109, 3521–3534.e6. 10.1016/j.neuron.2021.09.032. [PubMed: 34644546]
40. Ranade S, Hangya B, and Kepecs A. (2013). Multiple Modes of Phase Locking between Sniffing and Whisking during Active Exploration. *J. Neurosci.* 33, 8250–8256. 10.1523/JNEUROSCI.3874-12.2013. [PubMed: 23658164]
41. Ekstrom AD (2015). Why vision is important to how we navigate. *Hippocampus* 25, 731–735. 10.1002/hipo.22449. [PubMed: 25800632]
42. Muller A, Garren JD, Cao K, Peterson MA, and Ekstrom AD (2023). Understanding the encoding of object locations in small-scale spaces during free exploration using eye tracking. *Neuropsychologia*, 108565. 10.1016/j.neuropsychologia.2023.108565.
43. Ekstrom A, Viskontas I, Kahana M, Jacobs J, Upchurch K, Bookheimer S, and Fried I. (2007). Contrasting roles of neural firing rate and local field potentials in human memory. *Hippocampus* 17, 606–617. 10.1002/hipo.20300. [PubMed: 17546683]

44. Pastalkova E, Itskov V, Amarasingham A, and Buzsáki G. (2008). Internally generated cell assembly sequences in the rat hippocampus. *Science* 321, 1322–1327. 10.1126/science.1159775. [PubMed: 18772431]
45. Cantero JL, Atienza M, Stickgold R, Kahana MJ, Madsen JR, and Kocsis B. (2003). Sleep-Dependent θ Oscillations in the Human Hippocampus and Neocortex. *J. Neurosci.* 23, 10897–10903. 10.1523/JNEUROSCI.23-34-10897.2003. [PubMed: 14645485]
46. BJORNESS TE, BOOTH V, and POE GR (2018). Hippocampal theta power pressure builds over non-REM sleep and dissipates within REM sleep episodes. *Arch Ital Biol* 156, 112–126. 10.12871/00039829201833. [PubMed: 30324607]
47. Hines M, Poulter S, Douchamps V, Pibiri F, McGregor A, and Lever C. (2023). Frequency matters: how changes in hippocampal theta frequency can influence temporal coding, anxiety-reduction, and memory. *Front Syst Neurosci* 16, 998116. 10.3389/fnsys.2022.998116. [PubMed: 36817946]
48. Long LL, Bunce JG, and Chrobak JJ (2015). Theta variation and spatiotemporal scaling along the septotemporal axis of the hippocampus. *Front Syst Neurosci* 9, 37. 10.3389/fnsys.2015.00037. [PubMed: 25852496]
49. Fox KCR, Foster BL, Kucyi A, Daitch AL, and Parvizi J. (2018). Intracranial Electrophysiology of the Human Default Network. *Trends in Cognitive Sciences* 22, 307–324. 10.1016/j.tics.2018.02.002. [PubMed: 29525387]
50. Jenkinson M, Bannister P, Brady M, and Smith S. (2002). Improved optimization for the robust and accurate linear registration and motion correction of brain images. *Neuroimage* 17, 825–841. 10.1016/s1053-8119(02)91132-8. [PubMed: 12377157]
51. Poppenk J, Evensmoen HR, Moscovitch M, and Nadel L. (2013). Long-axis specialization of the human hippocampus. *Trends in Cognitive Sciences* 17, 230–240. 10.1016/j.tics.2013.03.005. [PubMed: 23597720]
52. Benhamou S. (2004). How to reliably estimate the tortuosity of an animal's path:: straightness, sinuosity, or fractal dimension? *Journal of Theoretical Biology* 229, 209–220. 10.1016/j.jtbi.2004.03.016. [PubMed: 15207476]

- The 3–12 Hz hippocampal “theta” oscillation driven by movement and linked to navigation
- Yet, theta oscillations are also observed in humans during verbal memory processing
- Here, we tested whether navigation or memory was the primary driver of human theta
- Results showed greater prevalence of human hippocampal theta during memory

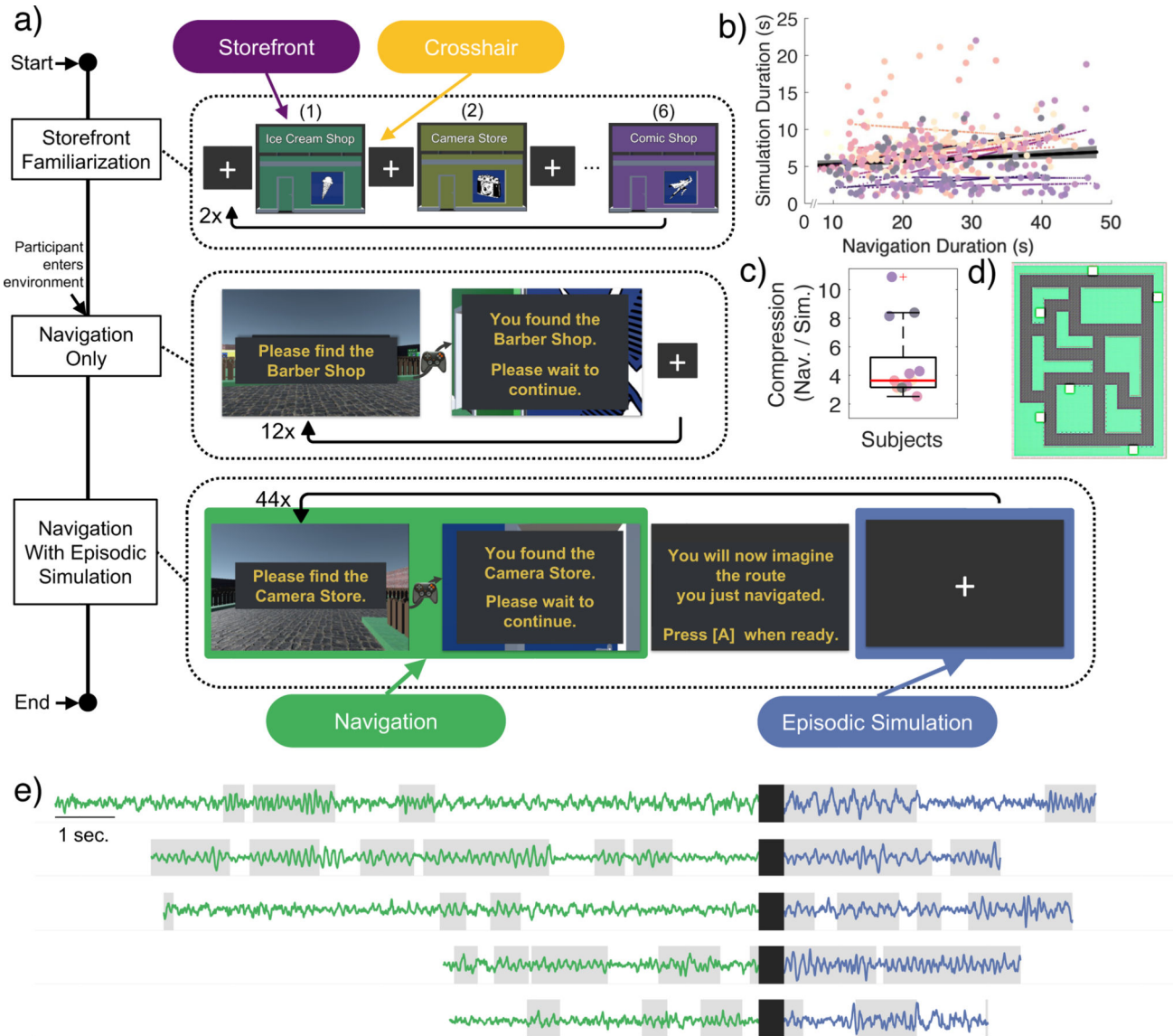


Figure 1:

Navigation task design, behavioral results, and iEEG traces.

a. Schematic of the experimental design. Store Familiarization– static images of each storefront were presented for 5000ms on a black background and followed by 5000ms of crosshair presentation; each storefront was presented 2x. Navigation Only– the subject was placed outside 1 of the 6 storefronts and used the XBox controller to locate the target store that was shown on the screen prompt (target store names remained visible at all times). Upon arrival at the proper target store, a 5000ms crosshair was presented before a new prompt appeared for the next target. The participants navigated to each store 2x. Navigation + Mental Simulation–similar to Navigation Only except, upon arrival at the proper target store, an on-screen prompt instructed participants to mentally navigate by picturing themselves at the starting location. Once prepared, the participants pressed [A] using the controller to start mental simulation and again once they imagined themselves outside the target destination.

- b. Scatter plot showing duration of navigation and duration of mental navigation for all trials for each patient. Distinct colors indicate individual patients, with the corresponding-colored lines representing the robust linear fit between navigation versus mental simulation durations for each patient. The thick black line shows the robust linear fit between navigation and mental navigation across data points for all patients.
- c. Across participants, the median rate of compression was significantly greater than 1 (Wilcoxon signrank $p < 0.001$, median navigation / replay = 3.43).
- d. Environment layout showing location of the 6 target stores.
- e. Example raw iEEG traces during navigation (green) and subsequent mental navigation (blue) for 6 representative examples. Gray shading indicates time points when the 2 – 12 Hz power exceeded the power of the 1/f background spectrum (see Methods).

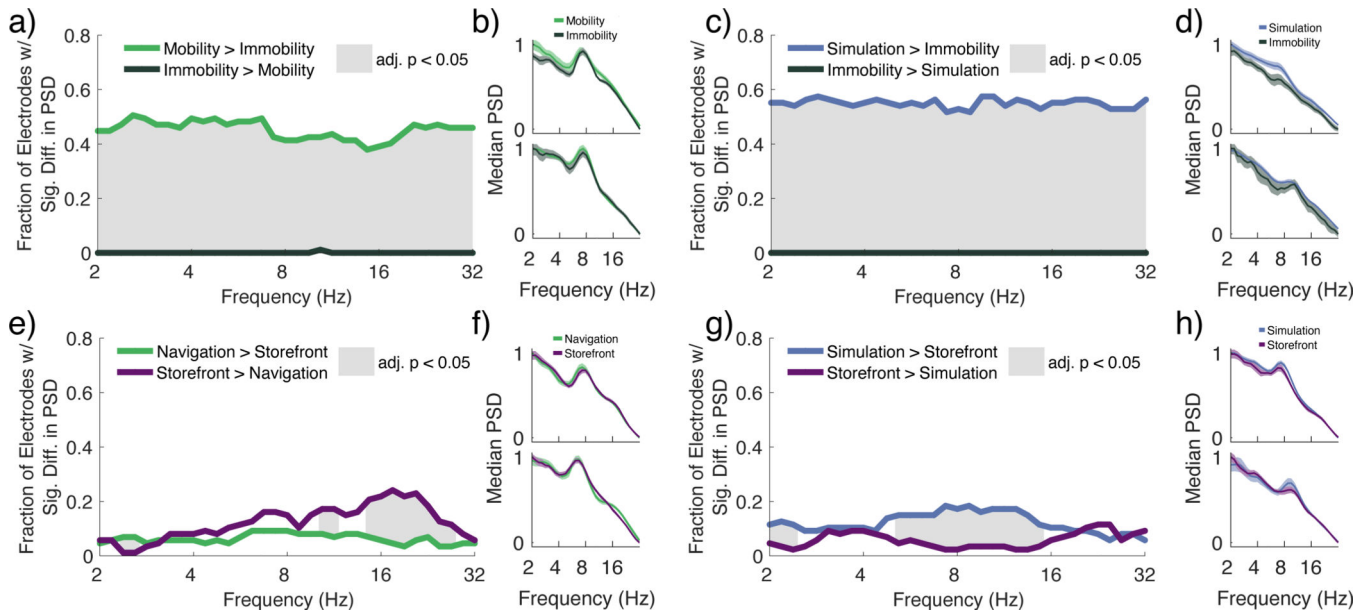


Figure 2:

Power spectral densities differ with memory demand, visual stimulation, and movement.

- a. Fraction of electrodes showing significantly greater power (ranksum FDR adjusted $p < 0.05$) during mobile versus immobile periods (green). No electrodes showed significantly greater power during immobility at any frequency. For all frequencies between 2–32Hz, the proportion of electrodes with significantly greater power during movement was significantly greater than the amount expected by chance (FDR adjusted $p < 0.05$; gray shaded areas).
- b. Two representative electrodes showing the median and median absolute difference of power during mobile (green) and immobile periods (dark green).
- c. Fraction of electrodes showing significantly different power during mental simulation versus immobile periods (sign-rank FDR adjusted $p < 0.05$). For all frequencies between 2 – 32Hz, the proportion of electrodes with significantly greater power during mental simulation (blue) was significantly greater than the amount expected by chance (FDR adjusted $p < 0.05$; gray shaded areas).
- d. Two representative electrodes showing the median and median absolute difference of power during mental simulation (blue) and immobility during the navigation condition (dark green).
- e. Fraction of electrodes showing significantly different power during mobile periods in the navigation condition versus storefront viewing (sign-rank FDR adjusted $p < 0.05$). From 2.4 – 3.1 Hz, the proportion of electrodes with significantly greater power during navigation (purple) was significantly greater than the amount expected by chance. For frequencies between 14.6 – 19 Hz, the proportion of electrodes with significantly greater power during storefront viewing (purple) was significantly greater than the amount expected by chance (FDR adjusted $p < 0.05$; gray shaded areas).
- f. Two representative electrodes showing the median and median absolute difference of power during the navigation condition (green) and storefront viewing (purple).
- g. Fraction of electrodes showing significantly different power during mental simulation versus storefront viewing (ranksum FDR adjusted $p < 0.05$). For frequencies 2.0 – 2.4 Hz

and 5.2 – 14.6 Hz, the proportion of electrodes with significantly greater power during mental simulation (blue) compared to storefront viewing was significantly greater than the amount expected by chance (FDR adjusted $p < 0.05$; gray shaded areas).

h. Two representative electrodes showing the median and median absolute difference of power during mental simulation (blue) and storefront viewing (purple).

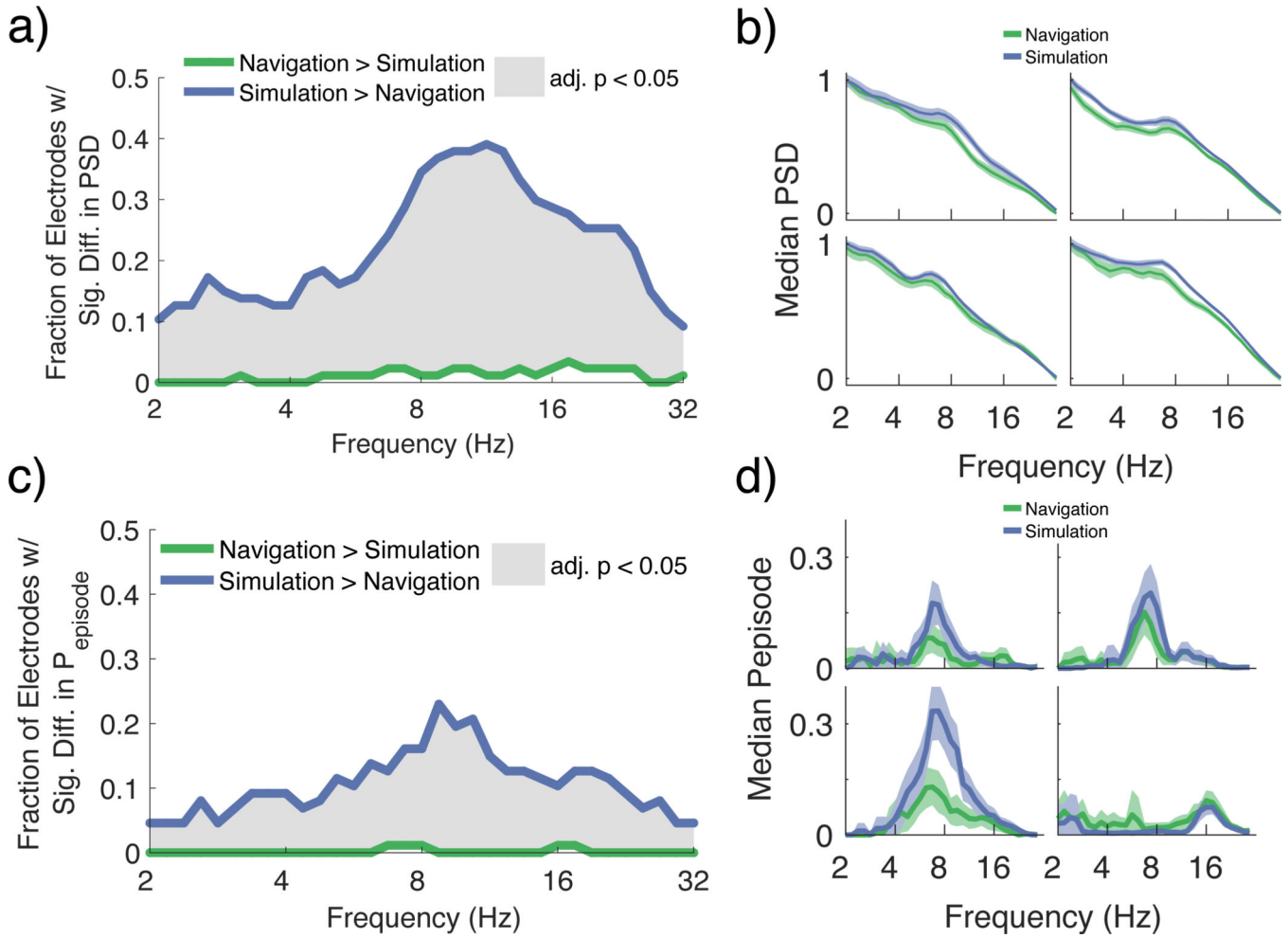


Figure 3:

Mental simulation results in greater low frequency activity than periods of mobility during the navigation condition.

- Fraction of electrodes showing significantly different power during navigation versus mental simulation (signrank FDR adjusted $p < 0.05$). For all frequencies between 2–32Hz, the proportion of electrodes with significantly greater power during mental simulation compared to navigation (blue) relative to the proportion of electrodes showing significantly greater power during navigation relative to mental simulation (green) was significantly greater than the amount expected by chance (FDR adjusted $p < 0.05$; gray shaded areas).
- Four representative electrodes showing the median and median absolute difference of power during navigation (green) and mental simulation (blue).
- Fraction of electrodes showing significantly different $P_{episode}$ during navigation versus mental simulation (signrank FDR adjusted $p < 0.05$). For all frequencies between 2–32Hz, the proportion of electrodes with significantly more oscillatory activity during mental simulation compared to navigation was significantly greater than the amount expected by chance (FDR adjusted $p < 0.05$; gray shaded areas).
- Four representative electrodes showing average $P_{episode}$ during navigation (green) and mental simulation (blue).

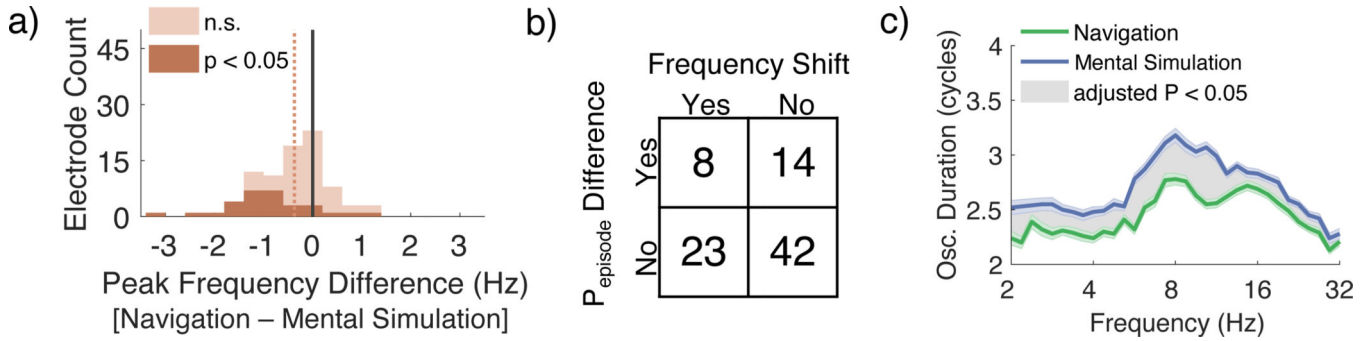


Figure 4:

Mental navigation induces higher frequency, longer duration, and greater power oscillations than navigation that cannot be accounted for by a broad-band frequency shift

a. Histogram showing the median trial level difference in peak frequency for navigation and mental simulation for all electrodes. The dark orange color represents the subset of electrodes whose frequency difference was significantly different from zero when tested across trials (Wilcoxon signrank $p < 0.05$); light orange indicates all electrodes. Across all electrodes, the median trial level frequency difference was significantly different than zero (Wilcoxon signrank $p < 0.0001$); leftward skew of the distributions indicates simulation frequency $>$ navigation frequency.

b. Contingency table showing the number of electrodes that had a significant difference in the trial-level peak frequency for navigation and simulation and the number of electrodes that had significant differences in the P_{episode} for navigation and mental simulation in the 2 – 12 Hz range. The P_{episode} differences between mental simulation and navigation are not significantly associated with a shift in the peak frequency between conditions (Fisher exact test $p = 1.000$).

c. Plot showing the median oscillation duration during navigation and mental simulation for frequencies 2 – 32 Hz. The median cycle duration across all frequencies between 2 – 32 Hz range was significantly greater during simulation than navigation (Wilcoxon signrank FDR adjusted $p < 0.05$).

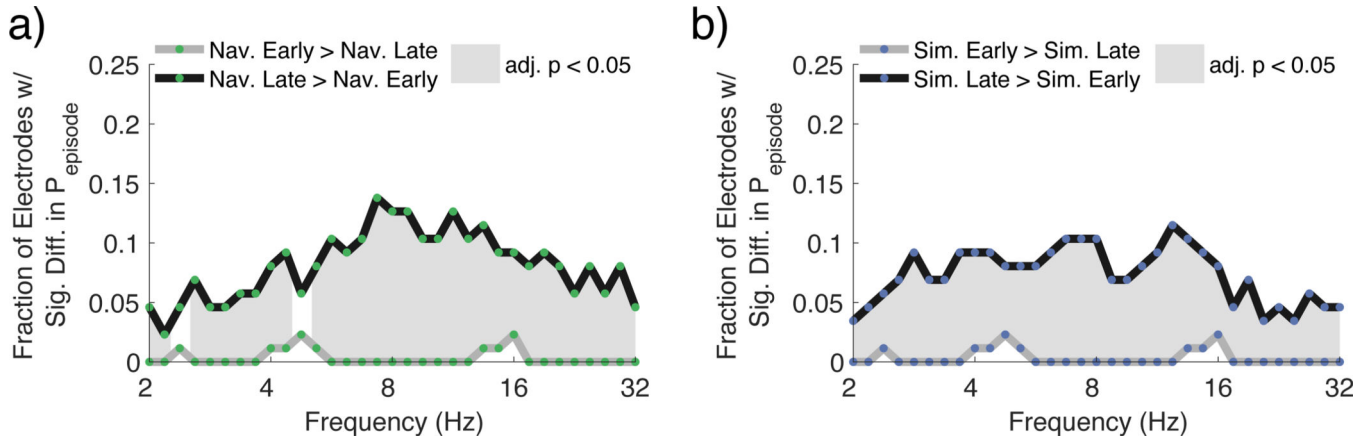


Figure 5:

Learning results in a greater prevalence of low frequency oscillations during navigation and mental simulation

a. Fraction of electrodes showing significantly different $P_{episode}$ during early versus late navigation trials (ranksum FDR adjusted $p < 0.05$). For all frequencies between 2 – 32 Hz except at 2.4 Hz and 4.8 Hz, the proportion of electrodes with significantly more oscillatory activity during late navigation compared to early navigation was significantly greater than the amount expected by chance (FDR adjusted $p < 0.05$; gray shaded areas).

b. Fraction of electrodes showing significantly different $P_{episode}$ during early versus late mental simulation trials (ranksum FDR adjusted $p < 0.05$). For all frequencies between 2 – 32 Hz, the proportion of electrodes with significantly more oscillatory activity during late mental simulation compared to early mental simulation (ranksum FDR adjusted $p < 0.05$) was significantly greater than the amount expected by chance (FDR adjusted $p < 0.05$; gray shaded areas).

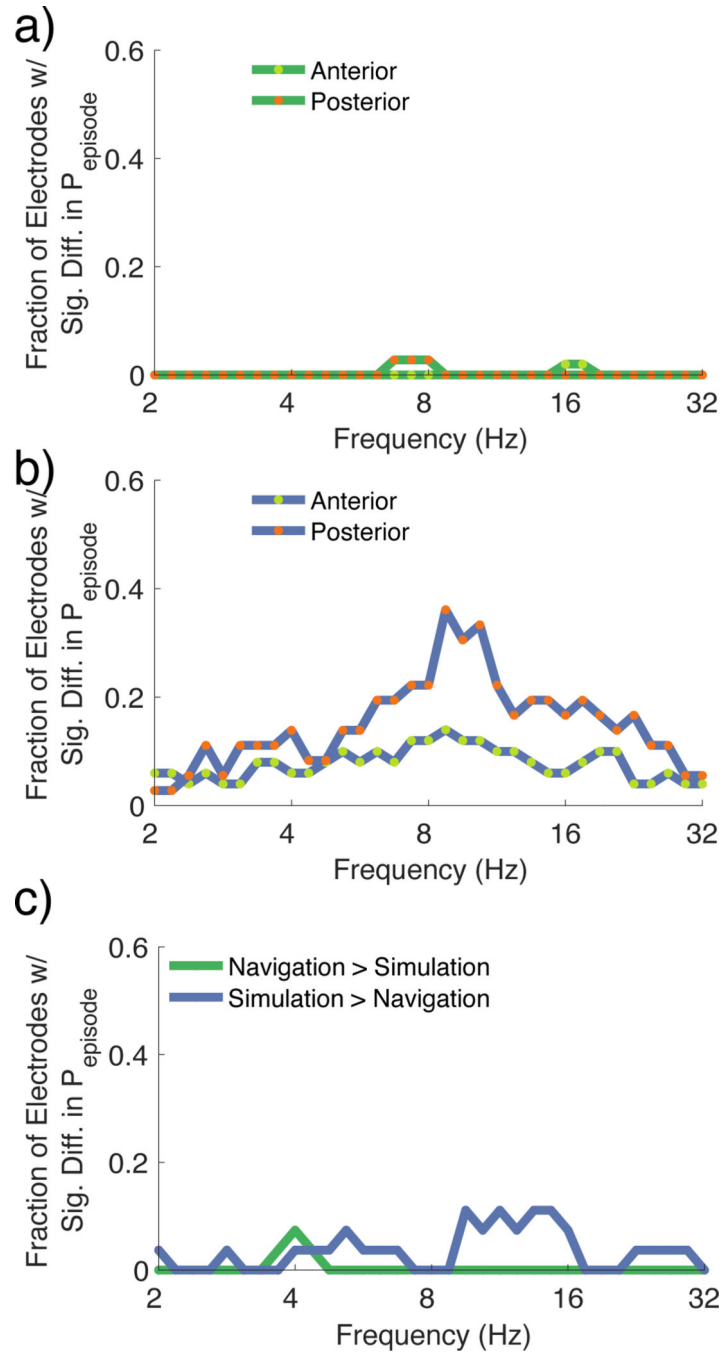


Figure 6: Low frequency differences for anterior versus posterior hippocampus and control analysis in anterior cingulate cortex
a. Fraction of electrodes with significantly greater power during navigation compared to mental simulation (Wilcoxon signrank FDR adjusted $p < 0.05$) plotted separately for the anterior (green) and the posterior hippocampus (orange). There were no frequencies at which the proportion of electrodes that showed significantly greater power during navigation

> mental simulation was significantly different in the anterior versus posterior hippocampus (FDR adjusted $p > 0.05$).

b. Fraction of electrodes showing significantly greater power during mental simulation compared to navigation (Wilcoxon signrank adjusted $p < 0.05$) plotted separately for the anterior and the posterior hippocampus. There were no frequencies at which the proportion of electrodes that showed significantly greater power during navigation > mental simulation differed for the anterior versus the posterior hippocampus (FDR adjusted $p > 0.05$).

c. Fraction of electrodes from the anterior cingulate cortex electrodes showing significantly different P_{episode} during navigation versus mental simulation (signrank FDR adjusted $p < 0.05$). For all frequencies between 2–32Hz, there was no significant difference in the proportion of electrodes showing greater power during navigation or mental simulation than the amount expected by chance (FDR adjusted $p > 0.05$).

KEY RESOURCES TABLE

REAGENT or RESOURCE	SOURCE	IDENTIFIER
Software and Algorithms		
extended Better Oscillation Detection Algorithm (eBOSC)	Whitten et al., 2011 and Hughes et al., 2012	https://doi.org/10.5281/zenodo.4668502
Deposited Data	N/A	https://doi.org/10.5281/zenodo.8058006

Author Manuscript

Author Manuscript

Author Manuscript

Author Manuscript